Robust Environmental Mapping by Mobile Sensor Networks: A Bayesian Method

Hyongju Park[1], Jinsun Liu[2], Matthew Johnson-Roberson[3] and Ram Vasudevan[1]

***Abstract*— Constructing a spatial map of environmental parameters is crucial step to prevent hazardous chemical leakage, forest fires, or to estimate the spatially distributed physical quantities, e.g., terrain elevation/radiation. Although previous methods can do such mapping tasks efficiently via dispatching a group of autonomous agents, the satisfactory convergence to the true distribution is guaranteed only when none of the robots/sensors/agents fail. A broad class of hardware and software failures are, however, commonly found in real-world applications, and will not only undermine overall mapping performance but could be critical to human safety as well. This paper presents a Bayesian approach for estimating an environmental parameters by deploying a group of mobile robots capable of ad-hoc communication equipped with short-range sensors. The topological (locations) and spatial properties (e.g., radiation level, magnetic field strength, temperature levels, etc), which constitute the target state are unknown and are characterized by a prior probability distribution over bounded domain. To this end, we present a general framework for coordinated multi-agent deployment aimed for good/better mapping performance [even when some part of the sensors fail]. First, for efficient robot-target assignment, we utilize the higher order Voronoi diagram where workspace is partitioned into disjoint regions and each region is associated with least one robots. Then, robots will be deployed to maximize the likelihood that at least one robot detects every targets in their associated region. A suite of simulation results is presented to demonstrate the effectiveness and robustness of the proposed method compared to existing methods.**

I. Introduction

A team of mobile robots equipped with ad-hoc communication and sensing devices, a *Mobile Sensor Network* (MSN), has a wide range of potential applications, including, exploration, surveillance, search and rescue missions, environmental monitoring for pollution detection and estimation, target tracking, cooperative detection of hazardous materials in contaminated environments, forest fire monitoring, oceanographic modeling, etc. [1]–[3]. Each such application can in fact be cast as a problem of trying to estimate some unknown, spatially distributed target of interest given some *a priori* measurement. Despite the fact that there are considerable efforts to achieve environmental mapping via MSNs, e.g., [4]–[6], there [are no known] methods that are able to provide [formal] guarantees under [sensor failure, e.g., erroneous sensor readings.] This paper aims to develop a class of sensing and motion model for MSNs to autonomously and collectively obtain an accurate representation of an arbitrary environmental map insensitive to failures under the Bayesian framework.

As a motivating example, consider the following scenario: a team of unmanned vehicles is deployed to monitor the radiation levels over a region of interest. Each vehicle is equipped with a range-limited noisy radiation sensor, to inspect the radiation level over the region of interest. The vehicles must approach the radiation sources close enough to ensure detection of the source while collectively building a radiation map over the entire region. To perform the required mission, the group of vehicles must solve two problems: (i) *robust deployment*: the vehicles must be able to distribute themselves to maximize the likelihood that the fleet can detect the target distributed over the bounded region. Thus, the collective measurements can be effectively combined to estimate the true target distribution; and (ii) *map construction*: robots must be able to effectively update their posterior map using the prior believe on the map and new observations retrieved at the current configuration. *The objective of this paper is to design a robust deployment and effective environmental map building strategy for the robotic network*. This focuses on a group of homogeneous mobile robots equipped with range sensors tasked with building a environmental map of a bounded domain where the data and the spatial coordinates of the data are correlated (e.g., precipitation map, heat distribution, radiation map, etc). This paper presents a novel sensor model along with a class of robust multi-robot deployment strategies under Bayesian framework, and an approximate method via Particle Filtering for efficient environmental map reconstruction.

Bayesian inference has guided the development of a variety of tools to recursively estimate the state of a dynamical system and has [, as a result,] provided a powerful statistical tool to manage the uncertainties in every measurement. In particular, during mobile robot search and exploration, the Bayesian approach has enabled the construction of tools for the localization of targets [7], target tracking [8], POMDP planning [9], and source localization [10], [11] (e.g., aerosol, gas, sound, chemical plume, radiation sources). In this latter instance for example, the Bayesian approach led to the development of an autonomous search algorithm that maximized information gain to find a diffusive source [10]. [5], [6] studied the multi-agent environment mapping problem, where a mutual information gathering—utilize this idea of maximizing information gain—was used to control multiple robots to build a intensity map in a hazardous environment.

[1]Hyongju Park and Ram Vasudevan are with the Department of Mechanical Engineering, University of Michigan, Ann Arbor, MI, 48109 USA hjcpark,ramv@umich.edu.

[2]Jinsun Liu is with the Robotics Institute, University of Michigan, Ann Arbor, MI, 48109 USA jinsunl@umich.edu.

[3]Matthew Johnson-Roberson is with the Department of Naval Architecture and Marine Engineering, University of Michigan, Ann Arbor, MI, 48109 USA mattjr@umich.edu.

Especially. [5] considered probabilistic robot failure model where probability of failure of each robot depends on the distances between hazard and the robot. They utilized the history of robot failures to avoid hazardous areas. In our paper, we consider a broader class of sensor/robot failure scenarios than that considered in [5]. In our study, robot failure events do not necessarily depend on the distribution of environmental parameters, e.g., radiation level.

Others have employed a non-Bayesian method to perform target distribution mapping using a single mobile robot [12]. This approach focused on trying to detect and identify gas concentration that was continuously distributed over a space. In this instance, the diffusive sensor, which is typically used in environmental mapping, was only able to provide information about a relatively small area compared to their sonar or laser range scan counterparts. To overcome the limitation, the authors proposed a novel grid-mapped technique which used a Gaussian kernel to model the decreasing likelihood that a particular reading represents the true concentration with respect to the distance from the point of measurement. Despite the promising results, their method did not scale well in larger environment since it relied upon a single-robot that was deployed using a pre-specified Mowing pattern.

Similar to [6], this paper focuses on multi-robot probabilistic search for diffusive source using multi-robot deployment strategies [2]. While those studies of deployment assume a static, known prior topological target distribution, their goal is to find deployment policies that maximize the collective quantity of interest, e.g., Quality of Service (QoS), Signal-to-Noise Ratio (SNR). On the other hand, this presents a general framework for incremental reconstruction of spatially distributed target information map over a bounded region using new measurements made from a MSN, where sensors are dynamically reconfigured to maximize the most recent collective belief on the target distribution.

This paper's primary contributions are three fold: first, a probabilistic sensor model that incorporates joint target detection and spatial distribution estimation by a group of mobile sensors while capturing a key characteristic of the target detection task–the probability of seeing a target, monotonically decreases as a function of the distance between the sensor and the target, which is a typical characteristic of range sensors. Second, a class of deployment strategies ranging from decentralized to fully coordinated ones are proposed not only to maximize the information gain but to provides relative robustness as well, which existing methods, e.g., [6] are not capable of. Also, we minimize the additional sensing effort—required a the cost of robustness—by adopting a general space partitioning method from computational geometry. Lastly, a variation of the Sequential Importance Resampling (SIR) Particle Filter—which uses the joint observations and the updated configuration of the robots—is adopted to update the posterior belief on the target efficiently via approximation.

Organizations: The rest of the paper is organized as follows. Section II presents notation used in the remainder of the paper, formally defines the problem of interest, and reviews a recursive Bayesian filter tailored to the problem. Section III presents a probabilistic sensor model. Section III studies the partitioned based approach to deployment, and the modified version of the sensor model discussed in Section IV. The deployment strategy is formally presented in Section V. Section VI discusses an approximate belief update method via particle filters. The effectiveness of this deployment and belief update approach is evaluated via numerical simulations in Sections VII. Finally, Section VIII concludes the paper and proposes a number of future directions.

II. Method for Probabilistic Mapping

This section presents the notation used throughout the paper, the problem of interest, and the recursive Bayesian filter.

A. Notations and Our System Definition

Throughout the text, the italic bold font is used to describe random quantities, a subscript t indicates that the value is measured at time step t, and $\mathbb{Z}^+$ denotes nonnegative integers. Given a continuous random variable $\boldsymbol{x}$, if it is distributed according to a Probability Density Function (PDF), we denote it by $f_{\boldsymbol{x}}$. Given a discrete random variable $\boldsymbol{y}$, if it is distributed according to a Probability Mass Function (PMF), we denote it by $p_{\boldsymbol{y}}$. Consider a group of m mobile robots deployed in a workspace, i.e., ambient space, $\mathcal{Q} \subseteq \mathbb{R}^d$. This paper assumes $d = 1, 2, 3$ though the presented framework generalizes. Let $\mathbb{S} = \{(x, y) \in \mathbb{R}^2 \mid x^2 + y^2 = 1\}$ be a *circle*, then the state of m robots is the set of locations and orientations at time t, and it is represented as an m-tuple $x_t = (x_t^1, \ldots, x_t^m)$, where $x_t^i \in \mathcal{Q} \times \mathbb{S}$. We denote by the set $x_{0:t} \coloneqq \{x_0, \ldots, x_t\}$ the robot states up to time t. Given a pair of states (x_t, x_{t+1}), robots follow a way-point-based, continuous-time, deterministic motion model with dynamic constraints:

$$\dot{x}(l) = \mathrm{f}(x(l),\, u(l)),\;\; l \in [l_0,\, l_f] \tag{1}$$

with boundary conditions $x(l_0) = x_t$ and $x(l_f) = x_{t+1}$ where $u(t)$ is a control, t_0 is the *initial time*, and t_f is the *final time* which is free. Let $u_t^\star$ be the *optimal control policy*[1] which drives robots' state from x_t to x_{t+1} in minimum time under the dynamic (or kinematic) constraints. Similarly, let $u_{0:t}$ be the sequence of control policies up to time t. We define a *target* to be a physical object or some measurable quantity spatially distributed over a bounded domain. Let $\boldsymbol{z}$ be the *target state* which is a random vector. The target state consists of location, $\boldsymbol{q} \in \mathcal{Q}$, and information state (quantitative information about the target), $\boldsymbol{I} \in \mathcal{I} \subseteq \mathbb{R}$. The Cartesian product $\mathcal{Z} = \mathcal{Q} \times \mathcal{I}$ is the *target state space*. Let the $(m \times n)$-tuple $\boldsymbol{y}_t = ((\boldsymbol{y}_t^{i,1}, \ldots, \boldsymbol{y}_t^{i,n}))_{i=1}^m$ be observations recorded by m robots at time step t [where each $\boldsymbol{y}_t^{i,j} \in \mathcal{Z}$, and n is the dimension of the sensor input.] Let the set

[1] In the current context, the optimal control policy is a sequence of control inputs (in discrete time domain) or control path (in continuous time domain) governed by dynamics of the vehicle. On example of such optimal control policy can be generated by Linear-Quadratic Regulator (LQR) if the dynamics were linear.

$\boldsymbol{y}_{1:t} := \{\boldsymbol{y}_1, \dots, \boldsymbol{y}_t\}$ denote observations made by robots up to time t.

B. Problem Definition

[In our context, we say that sensor measurement of a target by a robot is *reliable*, if the target can be detected by the robot and one of its sensors correctly reports a normal reading, and *unreliable* otherwise. Let $\mathcal{F} \subseteq \{1, \dots, m\}$ be the index set of robots whose sensors' measurements are always unreliable.] let $\mathcal{L}(u_t)$ be the likelihood of the observations y_t reported by m robots at time t:

$$\mathcal{L}(u_t) := p(y_t \mid x_{0:t-1}, y_{1:t-1}, u_t, \mathcal{F}) \tag{2}$$

[which depends on u_t—the control policy of m robots between $t-1$ and t, $y_{1:t-1}$—the observations up to time $t-1$, $x_{0:t-1}$—robots' trajectories prior to time t, and the index set of faulty robots which are unknown to others.] Also, we note here that the target state has been marginalized out[2]. [Let $\mathcal{L}^+(u_t)$ be the likelihood of reliable sensor measurements (more details will be given in Section III). Then] the objective of [our] environmental mapping problem is to obtain a sequence of optimal control policies $(u_1^\star, u_2^\star, \dots)$, each solves:

$$u_t^\star = \arg\max \mathcal{L}^+(u_t), \qquad t = 1, 2, \dots, \tag{3}$$

where each optimal policy between two time steps $[t,\, t+1)$, namely, u_t is subject to the dynamic constraints given in (1). Obtaining the optimal policy u_t can be proven to be NP-Hard by reduction from a simpler [static locational optimization] problem, namely, *m-median problem*[3]. Thus, to overcome the computational complexity, we will consider a gradient descent (greedy) approach. [Let b_t represent a the posterior probability distribution of the target state at time t, and] let $b^\star$ be the *true posterior belief*[4] on the target state. To this end, we quantify the difference between the true posterior belief, $b^\star$ and an approximation using our method via the Kullback-Leibler (K-L) divergence. We demonstrate via our numerical simulation in Section VII that for a given $\epsilon > 0$ [and $\mathcal{F} \neq \emptyset$], there is a dynamically varied reasonably small $T > 0$ such that after a sequence of optimal policies, $(u_1, \dots, u_t)$ is applied, $t > T$ implies $D_{\mathrm{KL}}\left(b_t \| b^\star\right) < \epsilon$.

C. Recursive Bayesian Filter

We present an overview of the Bayesian filter, and the derivation of the filtering equations for our primary goal: environmental mapping by m robots. [Recall that $b_t(z)$ represent a *belief* on target {information, location} state at time $t \in \mathbb{Z}_{\geq 0}$, the posterior probability distribution of the target state described by a random vector $\boldsymbol{z} \in \mathcal{Z}$. Thus, b_t describes the environmental map of some bounded region at time t. The state of robots are assumed completely *known*.] In a similar manner, the belief of target information state $\boldsymbol{I}$ given the target located at q is given by:

$$\begin{aligned} &b_t(I \mid \boldsymbol{q} = q) \\ &= f_{\boldsymbol{I} \mid b_0, x_{0:t-1}, u_t \boldsymbol{y}_{1:t}, \boldsymbol{q}}\left(I \mid b_0, x_{0:t}, u_t, y_{1:t}, \boldsymbol{q} = q\right). \end{aligned} \tag{4}$$

where we denote the initial belief on target state by b_0. Note that $b_t(I \mid \boldsymbol{q} = q)$ depends on the initial belief b_0, the previous robot trajectories up until time $t-1$ where $t \in \mathbb{Z}^+$, control policy between t and $t-1$, u_t, and observations up to this point, $\boldsymbol{y}_{1:t}$.

If the probability distribution about the target location, namely $f_{\boldsymbol{q}}$ is known *a priori*, the belief on the complete target state $\boldsymbol{z}$ is:

$$\begin{aligned} b_t(z) &= f_{\boldsymbol{z} \mid b_0, x_{0:t-1}, u_t, \boldsymbol{y}_{1:t}}\left(z \mid b_0, x_{0:t-1}, u_t, y_{1:t}\right) \\ &= b_t(I \mid \boldsymbol{q} = q) f_{\boldsymbol{q}}(q). \end{aligned} \tag{5}$$

If there is no prior knowledge of the target information at the initial time, one can choose the prior distribution as the *uniform* density. The observation $\boldsymbol{y}_t$ is conditionally independent of b_0, $\boldsymbol{y}_{1:t-1}$, and $x_{0:t-2}$ when it is conditioned on $\boldsymbol{z}$ and x_t Applying *Bayes' Theorem*, (4) becomes:

$$b_t(I \mid \boldsymbol{q} = q) = \frac{f_{\boldsymbol{y}_t \mid \boldsymbol{z}, x_{t-1}, u_t}\left(y_t \mid \boldsymbol{z} = (I, \boldsymbol{q} = q), x_{t-1}, u_t\right) b_{t-1}(I \mid \boldsymbol{q} = q)}{f_{\boldsymbol{y}_t \mid \boldsymbol{q}, x_{t-1}, u_t}\left(y_t \mid \boldsymbol{q} = q, x_{t-1}, u_t\right)}$$

where $t \in \mathbb{N}$. One can simplify the likelihood function in the target information map by using this observation, which yields:

$$b_t(I \mid \boldsymbol{q} = q) = \eta_t\, f_{\boldsymbol{y}_t \mid \boldsymbol{z}, x_{t-1}, u_t}\left(y_t \mid \boldsymbol{z} = (I, \boldsymbol{q} = q), x_{t-1}, u_t\right) b_{t-1}(I \mid \boldsymbol{q} = q) \tag{6}$$

where

$$\eta_t := \left(f_{\boldsymbol{y}_t \mid \boldsymbol{q}, b_0, x_{t-1}, u_t}\left(y_t \mid \boldsymbol{q} = q, b_0, x_{t-1}, u_t\right)\right)^{-1}$$

denotes the marginal probability, which is known as the *normalization constant*. This usually cannot be directly computed, but can be obtained by utilizing the total law of probability:

$$\begin{aligned} \eta_t = \Bigg(&\int_{\mathcal{I}} f_{\boldsymbol{y}_t \mid \boldsymbol{z}, x_{t-1}, u_t}\left(y_t \mid \boldsymbol{z} = (I, \boldsymbol{q} = q), x_{t-1}, u_t\right) \\ &\times b_{t-1}(I \mid \boldsymbol{q} = q)\, dI \Bigg)^{-1} \end{aligned} \tag{7}$$

By joining the (5) and (6), one can obtain a simplified form of the filtering equation:

$$\begin{aligned} b_t(z) &= \eta_t\, f_{\boldsymbol{y}_t \mid \boldsymbol{z}, x_{t-1}, u_t}\left(y_t \mid z, x_{t-1}, u_t\right) b_{t-1}(z) \\ &= \left(\prod_{i=1}^{t} \eta_i f_{\boldsymbol{y}_i \mid \boldsymbol{z}, x_{i-1}, u_i}\left(y_i \mid z, x_{i-1}, u_i\right)\right) b_0(z). \end{aligned} \tag{8}$$

We assume that m robots share their beliefs (this is similar to the concept of building mutual information map from [REFs]).

[2]Alternatively, one can also consider the *average* observation likelihood of all samples (targets) instead.

[3]m-median problem is one of the popular locational optimization problem where the objective is to locate m facilities to minimize the distance between demands and the facilities. The problem is NP-Hard in general graph (not necessarily a tree).

[4]We assume for now that the true posterior target distribution can be obtained, e.g., via exhaustive search and measurements made by a MSN.

III. Probabilistic Range-limited Sensor Model

Each mobile robot is equipped with a *range-limited sensor* that can measure quantitative information from afar and a *radio* to communicate with other nodes to share its belief. Each range sensor measurement is corrupted by noise, and the measurement is valid only if the target is detected. This combined sensor model joins the generic noisy sensor model with the binary detection model [13]. In fact, this combined sensor model has been experimentally validated during an object mapping and detection task using a laser scanner [14]. We postulate that this model is general enough to model other range-limited sensors as well; as long as the sensor is capable of distinguishing the target from the environment, and has uniform sensing range. A few example sensors satisfying these characteristics are 360-degree camera, wireless antenna, Gaussmeter, heat sensor, olfactory receptor, etc. While performing the detection task, we assume each sensor returns a 1 if a target is detected or 0 otherwise. The ability to detect a target for each i^{th} robot is a [binary] random variable $\boldsymbol{y}_D^i$ with a distribution that depends on the relative distance between the target and robot. This binary detection model, however, does not account for false positive or negatives. For example for a given $\mathcal{F}$, the probability of the event that all m sensors with configuration x_t fail to detect the target located at $q \in \mathcal{Q}$ with any intensity value is [

$$\begin{aligned} &p_{\boldsymbol{y}_{D,t}|x_{t-1},u_t,\boldsymbol{z},\mathcal{F}}\left(\boldsymbol{y}_{D,t}=\boldsymbol{0} \mid x_{t-1},u_t,\boldsymbol{z}=(q,I),\mathcal{F}\right) \\ &= p_{\boldsymbol{y}_{D,t}|x_{t-1},u_t,\boldsymbol{q},\mathcal{F}}\left(\boldsymbol{y}_{D,t}=\boldsymbol{0} \mid x_{t-1},u_t,\boldsymbol{q}=q,\mathcal{F}\right) \\ &= \prod_{i\in\mathcal{F}} p_{\boldsymbol{y}^i_{D,t}|x_{t-1},u_t,\boldsymbol{q}}\left(\boldsymbol{y}^i_{D,t}=0 \mid x_{t-1},u_t,\boldsymbol{q}=q\right) \end{aligned}$$

] where [$\boldsymbol{0}$ is a m-tuple of zeros]. For measuring a quantity of interest from a given environment, we consider a generic, noisy sensor model, where each sensor reports information regarding the environment, such as intensity data, as a *vector of reals*. Let $\boldsymbol{y}_t = (\boldsymbol{y}_t^1, \ldots, \boldsymbol{y}_t^n)$ be a n-random tuple for the measurements where n is the dimension of the sensor input. Without loss of generality, we assume that every random variable $\boldsymbol{y}_t^i$ has uniform *range* $[I_{\min}, I_{\max}]$ where, $I_{\min} \leq I_{\max}$ and $I_{\min}$, $I_{\max} \in \mathbb{R}$ for all $i \in \{1, \ldots, n\}$. According to our sensor model, the random vector $\boldsymbol{y}$ depends on $\boldsymbol{y}_D$ which is a [random] m-tuple corresponds to detection by m robots such that $\boldsymbol{y}_D = (\boldsymbol{y}_D^1, \ldots, \boldsymbol{y}_D^m)$ where $\boldsymbol{y}_D^i \in \{0, 1\}$ for all i when conditioned on $x_t, \boldsymbol{z}$, so that the conditional PDF can be computed as:

$$\begin{aligned} &f_{\boldsymbol{y}_t|\boldsymbol{z},x_{t-1},u_t,\mathcal{F}}(y_t \mid z, x_{t-1}, u_t, \mathcal{F}) \\ &= f_{\boldsymbol{y}_t|\boldsymbol{z},x_{t-1},u_t,\boldsymbol{y}_{D,t},\mathcal{F}}(y_t \mid z, x_{t-1}, u_t, \boldsymbol{y}_{D,t} \neq \boldsymbol{0}, \mathcal{F}) \\ &\quad \times p_{\boldsymbol{y}_{D,t}|\boldsymbol{z},x_{t-1},u_t,\mathcal{F}}(\boldsymbol{y}_{D,t} \neq \boldsymbol{0} \mid z, x_{t-1}, u_t, \mathcal{F}) \\ &+ f_{\boldsymbol{y}_t|\boldsymbol{z},x_{t-1},u_t,\boldsymbol{y}_{D,t},\mathcal{F}}(y_t \mid z, x_{t-1}, u_t, \boldsymbol{y}_{D,t} = \boldsymbol{0}, \mathcal{F}) \\ &\quad \times p_{\boldsymbol{y}_{D,t}|\boldsymbol{z},x_{t-1},u_t,\mathcal{F}}(\boldsymbol{y}_{D,t} = \boldsymbol{0} \mid z, x_{t-1}, u_t, \mathcal{F}), \end{aligned}$$

where $\boldsymbol{y}_D \neq \boldsymbol{0}$ means there is $j \in \{1, \ldots, m\}$ such that $\boldsymbol{y}_D^j = 1$ and $\boldsymbol{y}_D = \boldsymbol{0}$ means $\boldsymbol{y}_D^j = 0$ for all $j \in \{1, \ldots, m\}$. If target is missed-detected, i.e., $\boldsymbol{y}_{D,t} = \boldsymbol{0}$, the measurement is random which is modeled by uniform density, i.e., [

$$\begin{aligned} &f_{\boldsymbol{y}_t|\boldsymbol{z},x_{t-1},u_t,\boldsymbol{y}_{D,t},\mathcal{F}}(y_t \mid z, x_{t-1}, u_t, \boldsymbol{y}_{D,t} = \boldsymbol{0}, \mathcal{F}) \\ &= f_{\boldsymbol{y}_t|\boldsymbol{z},x_{t-1},u_t,\boldsymbol{y}_{D,t}}(y_t \mid z, x_{t-1}, u_t, \boldsymbol{y}_{D,t} = \boldsymbol{0}) \\ &= I_{\text{range}}^{-1} \end{aligned}$$

] where $I_{\text{range}} := I_{\max} - I_{\min}$. Also, we note by the law of total probability that

$$\begin{aligned} &p_{\boldsymbol{y}_{D,t}|\boldsymbol{z},x_{t-1},u_t,\mathcal{F}}(\boldsymbol{y}_{D,t} = \boldsymbol{0} \mid z, x_{t-1}, u_t, \mathcal{F}) \\ &= 1 - p_{\boldsymbol{y}_{D,t}|\boldsymbol{z},x_{t-1},u_t,\mathcal{F}}(\boldsymbol{y}_{D,t} \neq \boldsymbol{0} \mid z, x_{t-1}, u_t, \mathcal{F}). \end{aligned}$$

Then, we have:

$$\begin{aligned} &f_{\boldsymbol{y}_t|\boldsymbol{z},x_{t-1},u_t,\mathcal{F}}(y_t \mid z, x_{t-1}, u_t, \mathcal{F}) \\ &= (1 - p_{\boldsymbol{y}_{D,t}|\boldsymbol{z},x_{t-1},u_t,\mathcal{F}}(\boldsymbol{y}_{D,t} = \boldsymbol{0} \mid z, x_{t-1}, u_t, \mathcal{F})) \\ &\quad \underbrace{\times f_{\boldsymbol{y}_t|\boldsymbol{z},x_{t-1},u_t\boldsymbol{y}_{D,t},\mathcal{F}}(y_t \mid z, x_{t-1}, u_t, \boldsymbol{y}_{D,t} \neq \boldsymbol{0}, \mathcal{F})}_{\text{(a) Likelihood of reliable measurements}}, \\ &+ \underbrace{I_{\text{range}}^{-1} p_{\boldsymbol{y}_{D,t}|\boldsymbol{z},x_{t-1},u_t,\mathcal{F}}(\boldsymbol{y}_{D,t} = \boldsymbol{0} \mid z, x_{t-1}, u_t, \mathcal{F})}_{\text{(b) Likelihood of unreliable measurements}} \end{aligned} \tag{9}$$

We are merely interested in maximizing [marginal] likelihood of reliable measurements [where the target state z has been marginalized out].

IV. Robots-Target Assignment: A Partition-Based Approach

We consider a partitioned-based strategy where the workspace is partitioned into m disjoint regions, and each robot is assigned to a region where it confines its detections This so called partitioned-based strategy is common to multi-robot coverage problems [2], [15]–[17]. The most popular one is based on the Voronoi tessellations (see e.g., [2], which we call a *non-coordinated strategy*). There are, in fact more general methods, which partition the workspace into p regions and assign $k \in \{1, \ldots, m\}$ robots each region (note that if $k = m$, the method becomes *centralized*) [15]. By doing so, one can ensure that each target has a chance to be detected by at least one of the k sensors. This approach, which we call the *coordinated strategy*, can provide relative robustness by varying the value of k from 1 to m. Thus, if each sensor has an effective sensing range long enough to cover the whole workspace, utilizing all m sensors to detect every target in the workspace becomes the most desirable strategy.

A. The Optimal Partition

Consider m sensors and a workspace partition of $\mathcal{Q}$ into l disjoint regions, W such that $W = (W^1, \ldots, W^l)$, where $\cup_i W^i = \mathcal{Q}$, and $W^i \cap W^j = \emptyset$ for all i, j pairs with $i \neq j$. Suppose the target location is a random variable $\boldsymbol{z}$ with PDF $\phi : \mathcal{Q} \to \mathbb{R}_{\geq 0}$. For a given target $q \in \mathcal{Q}$, we define the probability that a sensor located at x can detect target, by using a real-valued function $h(\|q - x^i\|)$ as a probability measure[5], which is assumed to decrease monotonically as a

[5]For the numerical simulations purpose, we further assume that $h(\cdot)$ is continuously differentiable function non-increasing on its domain, and the image of h must be in $[0, 1]$ for it to be a probability measure.

function of the distance between the target and the i^{th} sensor. Consider a bijection ${}^kG$ that maps a region to a set of k-points where the pre-superscript k explicitly states that the region is mapped to exactly k points. Additionally we make the following definitions:

Definition 4.1 (An Order−k Voronoi Partition [18]): Let x be a set of m distinct points in $\mathcal{Q} \subseteq \mathbb{R}^d$. The *order-$k$ Voronoi partition of $\mathcal{Q}$ based on x*, namely ${}^kV$, is the collection of regions that partitions $\mathcal{Q}$ where each region is associated with the k nearest points in x.

We also define another bijection ${}^kG^\star$ that maps a region to a set of k *nearest* points (out of x) to the region. The total probability that all m sensors fail to detect a target drawn by a distribution ϕ from $\mathcal{Q}$ is:

$$\int_{\mathcal{Q}} p_{\boldsymbol{y}_D|x,\boldsymbol{q}}\left(\boldsymbol{y}_D = \mathbf{0} \mid x, \boldsymbol{q} = q\right) \phi(q)\, dq. \tag{10}$$

By substituting $\mathcal{Q}$ with the workspace partition W, and $p_{\boldsymbol{y}_D|x,\boldsymbol{q}}\left(\boldsymbol{y}_D = \mathbf{0} \mid x, \boldsymbol{q} = q\right)$ with likelihood function h, we have

$$\begin{aligned} &H(x, W, {}^kG) \\ &= \sum_{j=1}^{l} \int_{W^j} \left(\prod_{x^i \in {}^kG(W^j)} \left(1 - h\left(\left\|q - x^i\right\|\right)\right) \right) \phi(q)\, dq \end{aligned} \tag{11}$$

where we note again that the joint missed-detection events are conditionally independent, if conditioned on x. In fact, the order-k Voronoi tessellation is the optimal workspace partition which minimizes H for each choice of x and k:

Theorem 4.1 ([17]): For a given x and k, $H(x, {}^kV, {}^kG^\star) \leq H(x, W, {}^kG)$ for all W, ${}^kG$.

Note that the order-k Voronoi partition V_k, along with the map $G_k^\star$ are uniquely determined given x, ϕ, and $\mathcal{Q}$.

B. Distributed Target Detection

This section presents a practical sensor model that is suited to *distributed* target detection. Our proposed sensor model utilizes the deterministic workspace partitioning method based on the classical order-k Voronoi partition toward the probabilistic sensor model presented in Section III. In addition, we introduce additional hard constraint for the model, namely the *effective sensing range*, $r_{\text{eff}} > 0$, to take into account the fact that each sensor has its own maximum sensing range. For a given k, and the target $z = (q, I)$, our range-limited binary detection model is:

$$\begin{aligned} &p_{\boldsymbol{y}^i_{D,t}|\boldsymbol{q},x_{t-1},u_t}\left(\boldsymbol{y}^i_{D,t} = 1 \mid, x_{t-1}, u_t, \boldsymbol{q} = q\right) \\ &= \begin{cases} h\left(\left\|q - x^i_t\right\|\right) & \text{if } q \in {}^kG^\star_t(x^i_t) \cap \mathcal{B}(x^i_t, r_{\text{eff}}), \\ 0, & \text{otherwise,} \end{cases} \end{aligned}$$

where $\mathcal{B}(x, r)$ is an open ball with radius r centered at x.

V. Robust Deployment

[Through deployment at each time, m robots try to maximize the observation likelihood under sensor failures. Since the set of robots with faulty sensors, whose index set $\mathcal{F}$, is unknown, we cannot solve to our problem which applied to all cases; however we could solve the minimax version of the problem, namely, to maximize the likelihood that at least one sensors can detect the target. The idea behind this is: by the robot-target assignment rule from Section (?), each target is assigned to k number of robots, and for up to $k-1$ faulty robots, there is at least one robot that can still detect a target. By promoting the probability that at least one sensor can detect the target, one can ensure a worst-case guarantee.]

Given the prior belief and the observations, robots compute/move their next way-points, and the posterior belief is updated at the new locations given the collected information. Using (9), we state the observation likelihood of positive detections as:

$$\begin{aligned} &\mathcal{L}^+(u_t) = \int_{\mathcal{Q}} \int_{\mathcal{I}} f_{\boldsymbol{y}_t|\boldsymbol{z},x_t}(y_t \mid (\boldsymbol{q} = q, I), x_t) b_{t-1}(I \mid \boldsymbol{q} = q)\, dI dq \\ &= \int_{\mathcal{Q}} \int_{\mathcal{I}} f_{\boldsymbol{y}_t|\boldsymbol{z},x_t,\boldsymbol{y}_{D,t},\mathcal{F}}(y_t \mid z, x_t, \boldsymbol{y}_{D,t} \neq \mathbf{0}, \mathcal{F}) \\ &\quad \times b_{t-1}(I \mid \boldsymbol{q} = q) f_{\boldsymbol{q}}(q)\, dI dq. \\ &- \int_{\mathcal{Q}} p_{\boldsymbol{y}_{D,t}|\boldsymbol{q},x_{t-1},u_t,\mathcal{F}}(\boldsymbol{y}_{D,t} = \mathbf{0} \mid \boldsymbol{q} = q, x_{t-1}, u_t, \mathcal{F}) \\ &\quad \times \int_{\mathcal{I}} f_{\boldsymbol{y}_t|\boldsymbol{z},x_{t-1},u_t,\boldsymbol{y}_{D,t},\mathcal{F}}(y_t \mid z, x_{t-1}, u_t, \boldsymbol{y}_{D,t} \neq \mathbf{0}, \mathcal{F}) \\ &\quad \times b_{t-1}(I \mid \boldsymbol{q} = q)\, dI f_{\boldsymbol{q}}(q)\, dq. \end{aligned} \tag{12}$$

Recall that at each t, we are interested in finding the optimal control policy u_t so as to drive robots to new configurations maximizing $\mathcal{L}^+(u_t)$ where $\mathcal{F} \subsetneq \{1, \ldots, m\}$. For a given $q \in \mathcal{Q}$, let

$$\begin{aligned} \widetilde{f}_{\boldsymbol{q}}(q) := &\int_{\mathcal{I}} f_{\boldsymbol{y}_t|\boldsymbol{z},x_{t-1},u_t,\boldsymbol{y}_{D,t},\mathcal{F}}(y_t \mid z, x_{t-1}, u_t, \boldsymbol{y}_{D,t} \neq \mathbf{0}, \mathcal{F})) \\ &\times b_{t-1}(I \mid \boldsymbol{q} = q)\, dI\, f_{\boldsymbol{q}}(q). \end{aligned}$$

Note that for a given k, by substituting $\widetilde{f}_{\boldsymbol{q}}$ with ϕ and x with x_t, the second term on the right hand side of (12) takes the identical form as $H(x, W, G^k)$ which was previously defined in (11). By using $\widetilde{f}_{\boldsymbol{q}}$, and (11), we define our cost function:

$$\begin{aligned} &\overline{\mathcal{L}}^+_k(u_t) \\ &= \sum_{j=1}^{l} \int_{W^j} \left(\prod_{x^i_t \in {}^kG(W^j_t)} \left(1 - h\left(\left\|q - x^i_t\right\|\right)\right), \right) \widetilde{f}_{\boldsymbol{q}}(q)\, dq \end{aligned} \tag{13}$$

where each x^i_t is obtained by forward dynamics from x^i_{t-1} via u^i_t. We note that for a given k, minimizing $\overline{\mathcal{L}}^+_k(u_t)$ implies maximizing $\mathcal{L}^+(u_t)$. Thus, our problem become

$$u^\star_t = \arg\min \overline{\mathcal{L}}^+_k(u_t), \tag{14}$$

subject to the vehicle dynamics (1). [If $\widetilde{f}_{\boldsymbol{q}}$ takes uniform density on $\mathcal{Q}$, then the physical meaning of the problem (14) is to find control law minimizing the probability that all robots fail to detect target over $\mathcal{Q}$ when k robots are assigned to each region, i.e., maximizing the probability that at least one robot can detect target over $\mathcal{Q}$. Due to the way we

posed the problem, if $k = n$, the solution to (14) guarantees maximum observation likelihood for up to $k - 1 = n - 1$ faults, whereas if $k = 1$, the solution does not provide any robustness guarantee even for a single faulty robot.] If h is differentiable, our deployment strategy can use the gradient: $\nabla \overline{\mathcal{L}}_k^+(u_t)$ to find the desirable control policy of the robots as described in Algorithm 1. [Also, due to the complexity of the problem], the Algorithm 1 uses coordinate gradient descent in cyclic fashion to obtain a sub-optimal solution, namely, $\hat{u}_t$ for each time t.

Algorithm 1: Gradient Algorithm (MMLE)

Input: $\overline{\mathcal{L}}_k^+$, f, $\hat{x}_{t-1}$, $\epsilon > 0$, $y_{D,t}, u_{t,0}$
Output: $\hat{u}_t$
$k \leftarrow 0$, $\Delta \leftarrow \epsilon$
while $\Delta > \epsilon$ **do**
  foreach $i \in \{1, \ldots, m\}$ **do**
    $u^i_{t,k+1} \leftarrow u^i_{t,k} - \alpha^i_{t,k} \nabla_i \overline{\mathcal{L}}_k^+(u_{t,k})$
    // $\alpha^i_{t,k}$ is obtained using a line search method
  $\Delta \leftarrow \overline{\mathcal{L}}_k^+(u_{t,k}) - \overline{\mathcal{L}}_k^+(u_{t,k+1})$
  $k \leftarrow k + 1$
$\hat{x}_t \leftarrow \hat{x}_{t-1} + u_{t,k}$
$\hat{u}_t \leftarrow$ LQR($\hat{x}_t$, $\hat{x}_{t-1}$, f)
return $\hat{u}_t$

Theorem 5.1: Algorithm 1 is convergent.
The formal proof of Theorem 5.1 is similar to the proof contained in our previous paper [17], and is thus omitted.

VI. Belief Approximation by Particle Filtering

We consider the Particle Filtering approach to reduce the complexity of the map reconstruction process.

A. Low Discrepancy Sampling

For our numerical simulations, we consider a low discrepancy sampling method, namely, Halton-Hammersley sequence, to sample continuously distributed targets in $z \in \mathcal{Z}$. This approach has been used for sampling-based algorithms for robot motion planning [19].

B. SIR Particle Filter

We consider Sequential Importance Resampling (SIR) [20] for the particle filtering process. For a given distribution on target locations, $f_{\boldsymbol{q}}(q)$, at each time t, based on the observations, the locations belief hypothesis is populated for N_1 samples initially generated with Halton-Hammersley sequence.

$$q^1, \ldots, q^{N_1} \tag{15}$$

where for each $i \in \{1, \ldots, N_1\}$, $j \in \{1, \ldots, N_2\}$,

$$\widetilde{w}_t^{ij} \propto f_{\boldsymbol{y}_t|\boldsymbol{z}_t, x_t}(y_t \mid \hat{x}_t, \boldsymbol{z} = (q^i, I^{ij})) \tag{16}$$

In a similar manner, for each sample q^i the information belief hypothesis is populated for N_2 samples from $\mathcal{I}$ initially generated by the Halton-Hammersley sequence. If we let $z_t^{ij} := (q^i, I_t^{ij})$, then the collection of $N := N_1 \times N_2$ tuples where each tuple is a particle-weight pair is

$$\left\{ \left\{ \left(z^{11}, \widetilde{w}_t^{11}\right), \ldots, \left(z^{1N_2}, \widetilde{w}_t^{1N_2}\right) \right\}, \left\{ \left(z^{21}, \widetilde{w}_t^{21}\right), \ldots, \left(z^{2N_2}, \widetilde{w}_t^{2N_2}\right) \right\}, \ldots, \left\{ \left(z^{N_1 1}, \widetilde{w}_t^{N_1 1}\right), \ldots, \left(z^{N_1 N_2}, \widetilde{w}_t^{N_1 N_2}\right) \right\} \right\}$$

where for each $i = 1, \ldots, N_1$, $\sum_{j=1}^{N_2} \widetilde{w}_t^{ij} = 1$.

After resampling and normalizing, the approximate posterior belief becomes

$$\hat{b}_t(z) = \sum_{k=1}^{N} w_t^k \delta(z - z^k) \tag{17}$$

which is a form of discrete random measure where the $w_t^1, \ldots, w_t^N$ are resampled, normalized weight such that $\sum_{k=1}^{N} w_t^k = 1$, and $\delta(z - z^k)$ is Dirac-delta function evaluate at z^k. The whole filtering process is depicted in Algorithm 2. Note that as discussed in previous studies [21], our particle filter uses standard re-sampling scheme to ensure the convergence of the mean square error toward zero with a convergence rate of $1/N_2$ for all $q \in \mathcal{Q}$.

Algorithm 2: Filtering Algorithm

Input: $\hat{b}_{t-1} = \{z^l, w_{t-1}^l\}_{l=1}^N, y_t, \hat{x}_{t-1}, I_{\text{range}}$
Output: $\hat{b}_t$
// Propogate motion model; see Algorithm 1
$\hat{u}_t \leftarrow$ MMLE($y_{D,t}$, $\hat{x}_{t-1}$)
// SIR Particle Filter
// 1) Update using the observation model
foreach $i \in \{1, \ldots, N_1\}$ **do**
  foreach $j \in \{1, \ldots, N_2\}$ **do**
    $\widetilde{w}_t^{ij} \leftarrow p_{\boldsymbol{y}_{D,t}|\boldsymbol{q}, \hat{x}_{t-1}, \hat{u}_t}(\boldsymbol{y}_{D,t} = \mathbf{0} \mid \boldsymbol{q} = q^i, \hat{x}_{t-1}, \hat{u}_t)(I_{\text{range}}^{-1} - w_{t-1}^{ij} f_{\boldsymbol{y}_t|\boldsymbol{z}, \hat{x}_{t-1}, \hat{u}_t, \boldsymbol{y}_{D,t}}(y_t \mid \boldsymbol{z} = z_t^{ij}, \hat{x}_{t-1}, \hat{u}_t, \boldsymbol{y}_{D,t} \neq \mathbf{0})) + w_{t-1}^{ij} f_{\boldsymbol{y}_t|\boldsymbol{z}, \hat{x}_{t-1}, \hat{u}_t, \boldsymbol{y}_{D,t}}(y \mid z, \hat{x}_{t-1}, \hat{u}_t, \boldsymbol{y}_{D,t} \neq \mathbf{0})$
// 2) Resample and Normalize
$\{w_t^l\}_{l=1}^N \leftarrow$ Resample($\{\widetilde{w}_t^l\}_{l=1}^N$, $\{w_{t-1}^l\}_{l=1}^N$)
return $\hat{b}_t \leftarrow \{z^l, w_t^l\}_{l=1}^N$
// Low Variance Resampling [22]
function Resample($\{\widetilde{w}_t^l\}_{l=1}^N$, $\{w_{t-1}^l\}_{l=1}^N$)
  forall $i \in \{1, \ldots, N\}$ **do**
    $\overline{w}_t^i \leftarrow \frac{\widetilde{w}_t^i \cdot w_{t-1}^i}{\sum_{i=1}^N \widetilde{w}_t^i \cdot w_{t-1}^i}$
  foreach $i \in \{1, \ldots, N_1\}$ **do**
    $\delta \leftarrow$ rand($(0; {N_2}^{-1})$)
    $cdf \leftarrow 0$, $k \leftarrow 0$, $c_j \leftarrow []$ for all j
    for $j = 0$, $j < N_2$ **do**
      $u \leftarrow \delta + j \cdot {N_2}^{-1}$
      while $u > cdf$ **do**
        $k \leftarrow k + 1$
        $cdf \leftarrow cdf + \overline{w}_t^{ik}$
      $c_{j+1} \leftarrow k$
    for $j = 1$; $j \leq N_2$ **do**
      $w_t^{ij} \leftarrow \frac{c_j}{N_2}$
  return $\hat{b}_t = \{z^l, w_t^l\}_{l=1}^N$

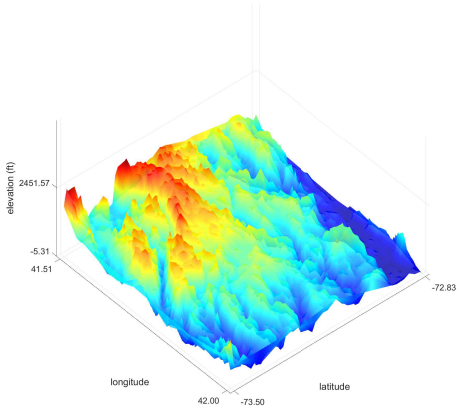

Fig. 1: Elevation map of some region in Connecticut (the ground truth)

VII. Numerical Simulations

This section presents a suite of numerical simulations to validate both our sensor model and a class of deployment strategies. In particular, we will focus on comparing our approach to popular state-of-the art approaches under various sensor failure scenarios.

Simulation settings: We consider $\mathcal{Q}$ be a unit rectangular space $[42.00, 41.51] \times [-73.49, -72.83]$ in $\mathbb{R}^2$, some mountain area in Connecticut, U.S.A, where each coordinate corresponds to latitude, longitude. We let $\mathcal{I} = [-1000,\ 4000]$ range of elevation in feet, and $r_{\text{eff}} = 2.89$ miles (or ∞ if it is relaxed). Targets are uniformly distributed over $\mathcal{Q}$, and the initial expected value for initial target information over $\mathcal{Q}$ is given in Fig. 1 as a mixture of Gaussian kernels. The information vector ranges from -1000 to 4000, i.e., $I_{\min} = -1000$, $I_{\max} = 4000$. It is assume that the robots have no prior knowledge of the target information. A number of particles used for the SIR filter is $N = N_1 \times N_2 = 5000 \times 100$. We consider Gaussian kernels for the probability distributions of both the perception model, and the detection model. The value of the equipped noisy sensor's covariance matrix is $\Sigma_I = 0.5\mathbf{I}$, and the binary sensor's covariance is $\Sigma_B = 0.04\mathbf{I}$ where $\mathbf{I} \in \mathbb{R}^{d \times d}$ is an identity matrix.

A. Convergence of our deployment algorithm

First, the behavior of the deployment strategy is discussed. Given the initial uniform prior belief and the initial configuration at x_0, robots is governed by the gradient descent strategy (Algorithm 1) to obtain the next way-point x_1 for the next time step 1. As previously noted in the Section V, robots are controlled to maximize the likelihood of reliable measurements. Fig. 2(a) shows the convergence of the algorithm, and Fig. 2(b) illustrates the path generated by optimal control policy when each robot is a unicycle.

B. Environmental mapping/filtering performance w/o failure

Next, we present the evolution of the object map given the uniform, initial map (Fig. 1) with successive positive observations, each followed by the gradient descent strategy

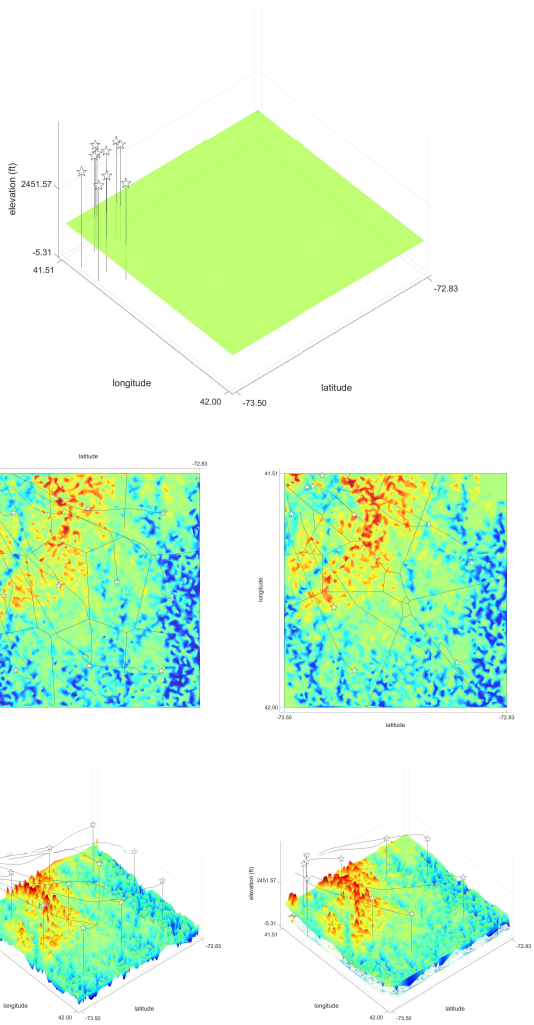

Fig. 2: One-time deployment with $k = 1$ (left), $k = 2$ (right), (a) Initial map, initial configuration, (b)-(c) robot configurations and map built after one-time deployment in 2D/3D (lines: gradient descent flow, circles: initial positions, stars: target positions, polygons: partition)

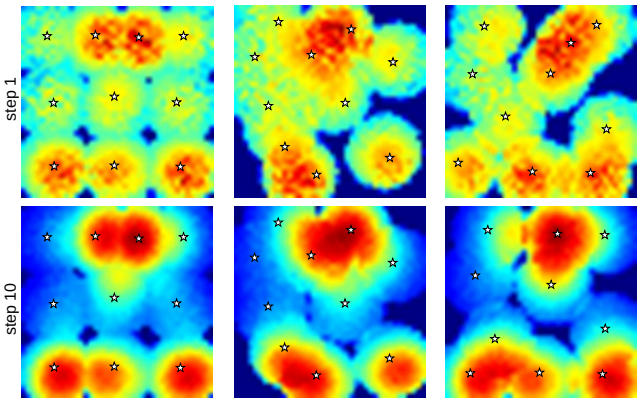

(a) $k = 1$ (b) $k = 2$ (c) $k = 10$

Fig. 3: Belief propagation using various methods with moderate detection range where $r_{\text{eff}} = 0.3$, $\Sigma_B = 0.04\mathbf{I}$, (a) $k = 1$, (b) $k = 2$, (c) $k = 10$, the 1st row: step 1, the 2nd row: step 10, stars: robots' positions at 10th step

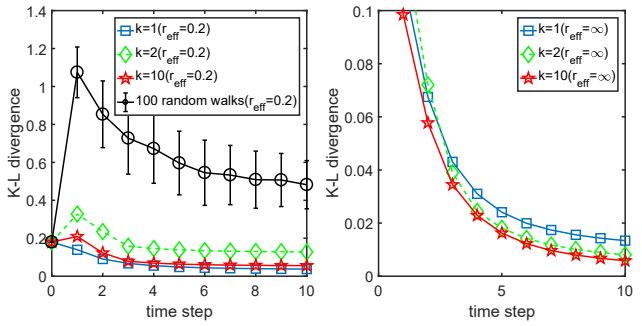

(a) (b)

Fig. 4: Comparison of K-L divergence from the actual distribution between different sensor models during belief propagation; (a) $r_{\text{eff}} = 0.2$, (b) $r_{\text{eff}} = \infty$

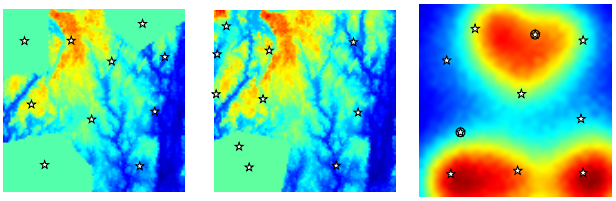

(a) $k = 1$ (b) $k = 2$ (c) $k = 10$

Fig. 5: Comparison of robots' configuration and beliefs at the final step with two approaches, $k = 1, 2, 10$ when two of the sensors fails (circled) and $r_{\text{eff}} = \infty$, $\Sigma_B = 0.04\mathbf{I}$ for both cases

and filtering process. Fig. 3 illustrates the map building process, given limited effective sensing range value ($r_{\text{eff}} = 0.2$, the value was chosen empirically relative to the workspace size) by different methods with $k = 1, 2, 10$ respectively, by showing robots' positions and the current belief at time step 1 and 10 respectively. The results in Fig. 3 clearly show that under *limited* sensing range, the non-coordinated strategy ($k = 1$) yields relatively better mapping results than coordinated strategies ($k = 2, 10$) compared to the ground truth map shown in Fig 1. Fig. 4(a) compares the K-L divergence values between different strategies during the evolution when $r_{\text{eff}} = 0.2$. We included the results with 2D random walks (100 walks) with step size 0.2 to illustrate the performance gain from our algorithm. Finally, Fig. 4(b) compares the K-L divergence values between different strategies when $r_{\text{eff}} = \infty$ merely to illustrate the filtering performance when the constraint on the sensing range is *relaxed*. As can be seen, in this case, coordinate strategies yields better performance than the the non-coordinate one. We also note that in all cases, our deployment strategies has noticeably improved the quality of the map along the evolutions. The occurrence of sudden jumps (between the time step 0 and 1) in the K-L divergence values observed in Fig 4(a) demonstrates the cases when the initial uniform density happened to a better '*guess*' than the crude belief obtained after a single propagation of the filtering process.

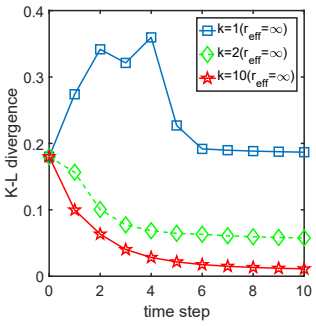

Fig. 6: Comparison of K-L divergence of the ground-truth between multiple strategies ($k = 1, 2, 10$), when two sensors fail during the evolution

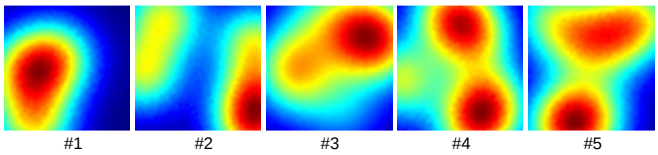

Fig. 7: Expected target intensities for 5 arbitrary environmental map

C. Robustness to sensor failure: benchmark comparison to existing methods

As seen in the previous section, despite the relatively higher sensing cost seen from the coordinated methods than the non-coordinated method, performances are even worse for the range-limited case. This section will present an example when coordinated strategies become more appealing which happens when the sensors are prone to fail. Results for robots configuration and target distributions after 10^{th} step with $k = 1, 2, 10$, are shown in Fig. 5(a)-(c), respectively. To reveal the full potential of the coordinated strategies, we relaxed the effective sensing range constraint such that, $r_{\text{eff}} = \infty$. As can be seen from Fig 5 and Fig. 6, the map retrieved by the coordinated strategies $k = 2, 10$ are more accurate/robust to the sensor failure compared to that obtained with the state-of-the-art Voronoi-based method. Due to its fully decentralized nature, it is not surprising to see from this example that the non-coordinated method ($k = 1$) works poorly under the sensor failures.

D. Sensitivity analysis: random initial configurations

Our method can be used to estimate arbitrary target distribution given randomly chosen initial configuration reasonably well. To show this, we consider five target distributions whose expected information densities are shown in Fig. 7. For each distribution, we ran our non-coordinated method ($k = 1$) with $r_{\text{eff}} = 0.2$. The mean and standard deviations of the K-L divergence of the ground truth and the reconstructed distribution at the 10^{th} beginning from 10 random configurations are summarized in Table I.

TABLE I: Mean and standard deviations (parenthesis) of K-L divergence for arbitrary distributions (Fig. 7) under 10 random initial configurations

Distribution type:	#1	#2	#3	#4	#5
K-L divergence	0.0358 (0.0034)	0.0308 (0.0033)	0.0495 (0.0041)	0.0293 (0.0012)	0.0339 (0.0024)

VIII. Conclusions and Future Work

This paper presents a general deployment strategy for autonomous fleet to maximize the recovery of environmental map over a bounded space, robots to sensor failures. It is expected that our method will fail if there is not enough number of mobile agents having sufficiently long effective sensing ranges compared to the workspace size. One of our future works is, therefore, to develop multi-agent patrolling algorithms (see e.g., [23]) to resolve such problems where there may not be enough sensors to cover the whole target space. Also, as reported in the literature [14], our combined sensor model has been adopted to emulate the real-world laser scanner's behavior, nevertheless, it is one of our future works to conduct extensive real world multi-robot experiments for further validation of our range sensor model. Lastly, we assumed in this study that the beliefs are shared between robots such that both tasks of information gathering, propagating and approximating belief require a central entity. In the future, we will explore how to devise distributed communication protocol to enable distributed belief estimation.

References

[1] S. S. Dhillon and K. Chakrabarty, "Sensor placement for effective coverage and surveillance in distributed sensor networks," in *Wireless Communications and Networking, 2003. WCNC 2003. 2003 IEEE*, vol. 3. IEEE, 2003, pp. 1609–1614.

[2] J. Cortés, S. Martínez, T. Karatas, and F. Bullo, "Coverage control for mobile sensing networks," *Robotics and Automation, IEEE Transactions on*, vol. 20, no. 2, p. 243255, 2004.

[3] L. Yu, N. Wang, and X. Meng, "Real-time forest fire detection with wireless sensor networks," in *Wireless Communications, Networking and Mobile Computing, 2005. Proceedings. 2005 International Conference on*, vol. 2. IEEE, 2005, pp. 1214–1217.

[4] D. Connor, P. Martin, and T. Scott, "Airborne radiation mapping: overview and application of current and future aerial systems," *International Journal of Remote Sensing*, vol. 37, no. 24, pp. 5953–5987, 2016.

[5] M. Schwager, P. Dames, D. Rus, and V. Kumar, "A multi-robot control policy for information gathering in the presence of unknown hazards," in *Robotics Research*. Springer, 2017, pp. 455–472.

[6] R. A. Cortez, H. G. Tanner, R. Lumia, and C. T. Abdallah, "Information surfing for radiation map building," *International Journal of Robotics and Automation*, vol. 26, no. 1, p. 4, 2011.

[7] F. Bourgault, T. Furukawa, and H. F. Durrant-Whyte, "Coordinated decentralized search for a lost target in a bayesian world," in *Intelligent Robots and Systems, 2003.(IROS 2003). Proceedings. 2003 IEEE/RSJ International Conference on*, vol. 1. IEEE, 2003, pp. 48–53.

[8] L. D. Stone, R. L. Streit, T. L. Corwin, and K. L. Bell, *Bayesian multiple target tracking*. Artech House, 2013.

[9] S. Candido, J. Davidson, and S. Hutchinson, "Exploiting domain knowledge in planning for uncertain robot systems modeled as pomdps," in *Robotics and Automation (ICRA), 2010 IEEE International Conference on*. IEEE, 2010, pp. 3596–3603.

[10] B. Ristic, M. Morelande, and A. Gunatilaka, "Information driven search for point sources of gamma radiation," *Signal Processing*, vol. 90, no. 4, pp. 1225–1239, 2010.

[11] J.-M. Valin, F. Michaud, and J. Rouat, "Robust localization and tracking of simultaneous moving sound sources using beamforming and particle filtering," *Robotics and Autonomous Systems*, vol. 55, no. 3, pp. 216–228, 2007.

[12] A. J. Lilienthal, M. Reggente, M. Trincavelli, J. L. Blanco, and J. Gonzalez, "A statistical approach to gas distribution modelling with mobile robots-the kernel dm+ v algorithm," in *Intelligent Robots and Systems, 2009. IROS 2009. IEEE/RSJ International Conference on*. IEEE, 2009, pp. 570–576.

[13] P. M. Djuric, M. Vemula, and M. F. Bugallo, "Target tracking by particle filtering in binary sensor networks," *IEEE Transactions on Signal Processing*, vol. 56, no. 6, pp. 2229–2238, 2008.

[14] D. Anguelov, D. Koller, E. Parker, and S. Thrun, "Detecting and modeling doors with mobile robots," in *Robotics and Automation, 2004. Proceedings. ICRA'04. 2004 IEEE International Conference on*, vol. 4. IEEE, 2004, pp. 3777–3784.

[15] S. Hutchinson and T. Bretl, "Robust optimal deployment of mobile sensor networks," in *Robotics and Automation (ICRA), 2012 IEEE International Conference on*, 2012, p. 671676.

[16] M. Schwager, D. Rus, and J.-J. Slotine, "Decentralized, adaptive coverage control for networked robots," *The International Journal of Robotics Research*, vol. 28, no. 3, pp. 357–375, 2009.

[17] H. Park and S. Hutchinson, "Robust optimal deployment in mobile sensor networks with peer-to-peer communication," in *Robotics and Automation (ICRA), 2014 IEEE International Conference on*. IEEE, 2014, pp. 2144–2149.

[18] M. I. Shamos and D. Hoey, "Closest-point problems," in *Foundations of Computer Science, 1975., 16th Annual Symposium on*. IEEE, 1975, pp. 151–162.

[19] S. M. LaValle, *Planning algorithms*. Cambridge university press, 2006.

[20] M. S. Arulampalam, S. Maskell, N. Gordon, and T. Clapp, "A tutorial on particle filters for online nonlinear/non-gaussian bayesian tracking," *IEEE Transactions on signal processing*, vol. 50, no. 2, pp. 174–188, 2002.

[21] D. Crisan and A. Doucet, "A survey of convergence results on particle filtering methods for practitioners," *IEEE Transactions on signal processing*, vol. 50, no. 3, pp. 736–746, 2002.

[22] H. M. Choset, *Principles of robot motion: theory, algorithms, and implementation*. MIT press, 2005.

[23] D. Portugal and R. Rocha, "A survey on multi-robot patrolling algorithms," in *Doctoral Conference on Computing, Electrical and Industrial Systems*. Springer, 2011, pp. 139–146.